ON THE KINEMATICS OF THE OCTOPUS'S ARM

Y. LEVINSON AND R. SEGEV

Abstract. The kinematics of the octopus's arm is studied from the point of view of robotics. A continuum three-dimensional kinematic model of the arm, based on a nonlinear rod theory, is proposed. The model enables the calculation of the strains in the various muscle fibers that are required in order to produce a given configuration of the arm—a solution to the inverse kinematics problem. The analysis of the forward kinematics problem shows that the strains in the muscle fibers at two distinct points belonging to a cross section of the arm determine the curvature and the twist of the arm at that cross section. The octopus's arm lacks a rigid skeleton and the role of material incompressibility in enabling the configuration control is studied.

1. Introduction

This paper presents a kinematical model for the octopus's arm. The arm of an octopus is an efficient hyper-redundant manipulator and hence the motivation for studying it. We focus on the kinematic analysis of a three dimensional continuum model. Of particular interest is the way the octopus uses the incompressibility of the arm to overcome the absence of a rigid skeleton.The following is a kinematical analysis that could suggest some applications in biomimetic robots. However, we do not consider specific applications to robots nor do we suggest technologies that may enable the construction of continuous robots having the kinematic model described below. A kinematic model of the octopus's arm having a finite number of degrees of freedom, and therefore, a lot simpler to implement, is presented in the first author's thesis [1].

In many cases, hyper-redundant robots are modeled as discrete mechanical systems, e.g., [2, 3, 4, 5]. Two-dimensional discrete kinematical and dynamical models for the octopus's arm are presented in [6] and [7]. In their study, the authors model the arm as an array of point masses interconnected by linear or non-linear springs that represent the muscles. The incompressibility constraint is applied by preserving the area of each compartment created by four adjacent masses. The model considers external forces, such as gravity, drag, buoyancy, and internal forces, such as the muscles' active forces and the forces needed to preserve the area of the compartments.

Following studies such as [8, 9] on continuous models for hyper-redundant robots, Boyer et al., [10], used a geometrically exact theory of non-linear

Date: September 9, 2009.

beams to simulate the dynamics of swimming of an eel-like robot. In their analysis the robot is treated as a continuous series of infinitesimal sections. The deformation is defined by a homogeneous matrix $\mathbf{g}$ that describes the orientation and translation of each section. The authors write the differential equation for the homogeneous transformations of the cross section along the axis of the arm, X, in the form,

$$\begin{bmatrix} \frac{\partial \mathbf{R}}{\partial X} & \frac{\partial \mathbf{d}}{\partial X} \\ 0 & 0 \end{bmatrix} = \begin{bmatrix} \mathbf{R} & \mathbf{d} \\ 0 & 1 \end{bmatrix} \begin{bmatrix} \hat{\mathbf{K}} & \mathbf{\Gamma} \\ 0 & 0 \end{bmatrix}.$$

Here, $\mathbf{R}$ is the orientation matrix for the cross-section, $\mathbf{d}$ is the position vector for the center of the cross-section, $\mathbf{\Gamma} = \mathbf{R}^{\mathrm{T}} \frac{\partial \mathbf{d}}{\partial X}$, and $\hat{\mathbf{K}} = \mathbf{R}^{\mathrm{T}} \frac{\partial \mathbf{R}}{\partial X}$ is a skew-symmetric matrix whose components describe the bending and torsion of the robot. The first component of $\mathbf{\Gamma}$ describes the stretching of the centerline of the robot; the two remaining components describe the shear of the sections relative to one another. The dynamic model considers the swimming locomotion and the affect of forces caused by the flow.

The present work is similar to Boyer et al. [10], as we also use a geometrically nonlinear continuum theory of rods. However, our kinematic analysis of the octopus's arm studies what seems to us to be an essential aspect of the control of its configuration, namely, the role of an incompressibility constraint. Specifically, it is assumed here that the volume of any segment of the arm (bounded between two cross sections) remains fixed during a deformation.

It is noted that the equations governing the mechanics of pointwise incompressible rods are formulated and solved by Antman [11]. Antman does not present any application and his work is concerned with the kinematics of the cross sections for pointwise incompressible rods. As mentioned, we use a simplified theory were incompressibility is assumed to hold only for segments of the arm rather than pointwise.

The present kinematical model describes the relative rotations of the cross sections due to bending and torsion. As an additional kinematic constraint, we adopt a traditional hypothesis of rod theory~~the Euler-Bernoulli hypothesis~~ and do not consider transverse shear of the various cross sections.

Our objective is to study the kinematics of the octopus's arm from the point of view of robotics, namely, the inverse kinematics problem and direct kinematics problem. Thus, one has to define what parameters of the arm's configuration should be controlled and what are the actuation parameters. Subject to the constraints of the three dimensional rod theory described, it is assumed here that it is necessary to control the configuration of the arm completely. In other words, rather than controlling a part of the arm, the analog of an end effector, the geometry of the entire centerline in space and the twist of the arm about it are considered. This requirement is motivated by the existence of suction units along the entire length of the arm. The actuation parameters are the strains in the various muscle fibers of the arm. Thus, for the inverse kinematics problem one seeks the strains in the various

muscle groups that will induce a required configuration of the arm. For the forward kinematics problem, one seeks the configuration of the arm induced by given strains in the muscle. An analysis of these two problems is presented in Section 5, following the introduction of the basic kinematic variables in Section 3 and the analysis of strain in Section 4.

2. Octopus's Arm Physiology: An Overview

Organs such as the mammalian tongue, the elephant's trunk and the octopus's arms are termed *Muscular Hydrostats* [12]. They are characterized by their lack of vertebras and compressible cavities. The most important feature of muscular hydrostats is their relatively large bulk modulus that results from a dense musculature without any gas-filled cavities or large blood vessels [13]. This enables manipulation of an organ lacking any vertebrate skeleton by activating two or more muscle group simultaneously.

The octopus's arm consists of three primary muscle fiber groups surrounding a central axial nerve cord (Figure 2.1): the longitudinal muscles, the transverse muscles and the oblique or helicoidal muscles. The latter appear in both a right handed coil and a left handed coil.

The transverse muscle fibers are oriented in planes perpendicular to the axis of the arm. They are laid in an orthogonal array surrounding the axial nerve cord. Two bundles extend parallel to the lateral plane,[1] and two bundles are parallel to the frontal plane (see Figure 3.1).

The longitudinal fibers surround the transverse fibers in four bundles, an oral bundle, an aboral bundle and two lateral bundles. The cross section area is larger in the aboral bundle, in comparison with the oral and lateral bundles. This enables the exertion of higher moments when the arm is bent aborally to reveal the suction line.

Helicoidal muscle fibers appear in three different layers: internal, median and external. In every cross section, the three layers (or groups) spiral around the centerline both in a right handed helix and a left handed helix. Kier and Stella examined in [13] two octopus's species and reported mean pitch angle of 62° for external and median oblique muscles fibers. Internal oblique muscles fibers have a lower mean pitch angle that varies between the two species: 42° for Octopus briareus and 56° for Octopus digueti.

As the arm does not contain any rigid skeleton, control of the configuration is made possible by combining incompressibility with contractions of a number of muscle groups. In addition, the incompressibility property compensates for the inability of the muscle fibers to extend actively. For example, due to volume conservation, the arm will extend passively when the transverse muscles are contracted actively.

As another example, a contraction of the longitudinal muscle at the oral side will cause shortening of the arm and an increase of the cross section area.

[1] Note that in order to show the suction elements clearly, the lateral plane is drawn vertically in Figure 3.1.

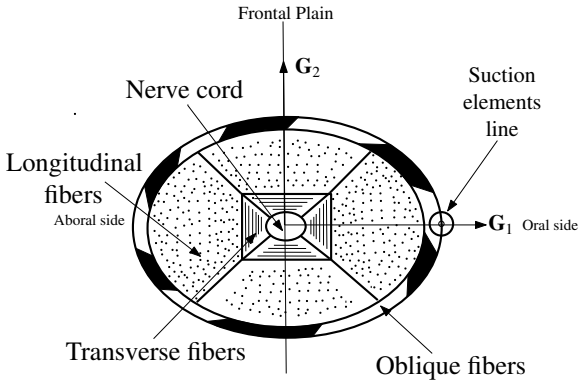

Figure 2.1: A schematic cross section of an octopus's arm.

To avoid the contraction and create flexure, the cross section area is held fixed by contracting the transverse muscles. As a result of the arm's inability to change its volume, the aboral side must elongate and thus produce flexure of the arm in the sagittal plane.

The role of the helicoidal muscle groups may be explained roughly as follows. Consider the arm in its straight unbent configuration. Assuming that the helicoidal muscles are in 45° to the centerline, extension of the right handed helicoidal fibers and contraction of the same magnitude of the left handed helicoidal fibers will produce the shear strain needed for the right handed twist of the arm—the strain needed for the "adjacent" cross section to turn right relative to the "current" cross section. In general, muscle fibers do not extend actively. In the situation described above, the right handed fibers extend because of volume conservation.

As mentioned in the introduction, our objective in the paper is to give a robot kinematics model of the octopus's arm. In such a model, the strains in the various muscle fiber groups make up the "joint variables". In such a model, for the inverse kinematics problem one computes the strains in the muscle fiber groups for a given configuration of the arm. In particular, the role of incompressibility is such a kinematic model will be studied.

3. Configurations of the Arm

3.1. **Notation and Preliminaries.** The reference configuration of the arm is assumed to be an elliptical cylinder in the vector space $\mathbb{R}^3$. Each material point in the arm is described by the reference coordinates $(X_1, X_2, X_3) = (X, Y, S)$ in some reference frame and it assumed that at the reference configuration, the centerline occupies the points $(0, 0, S)$ for $S \in [0, 1]$ with the base of the arm being located at $S = 0$. Thus, the centerline of the arm is situated along the $X_3 = S$ axis and is set to be of a unit length for the sake of simplicity. The principal axes of the elliptical cross section of the cylinder are denoted as a_0 and b_0 and are in the directions of the X and Y

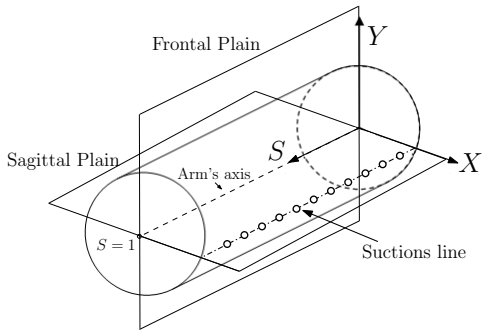

Figure 3.1: The reference configuration of the arm

coordinate axes, respectively. The suction elements are located on the points on the circumference of the cylinder for which $Y = 0$ and $X = a_0$ (see Figure 3.1).

The radius vector in the reference frame to typical material point of the arm is $\mathbf{R} = \mathbf{R}(X, Y, S)$ and the undeformed centerline curve will be denoted as $\mathbf{R}_0(S) = \mathbf{R}(0, 0, S)$. At each point in the reference state we may define the base vectors, $\mathbf{G}_p = \frac{\partial \mathbf{R}}{\partial X_p}$. As the reference configuration is a right cylinder, the vectors $\{\mathbf{G}_p\}$ are orthonormal and are identical to the unit vectors along the reference coordinate axes.

The actual configurations of the arm take place in the physical space which we do not necessarily identify with the reference frame. The physical space is represented by a 3-dimensional Euclidean space and it is assumed that a specific orthonormal frame is given. Thus, denoting the orthonormal base vectors by $\mathbf{e}_i$, $i = 1, 2, 3$, any point in space may be represented in the form $\mathbf{r} = x_i \mathbf{e}_i$, where summation on repeated indices is implied.

The deformed configuration of the arm is specified by a function $\mathbf{r} = \mathbf{r}(\mathbf{R}) = \mathbf{r}(X, Y, S)$ giving the position in space corresponding to each material point $\mathbf{R}$ at the deformed configuration so that $x_i = x_i(X_p)$. For simplicity, it is assumed that

Assumption 0. $\mathbf{r}(\mathbf{0}) = \mathbf{0}$*, and the points* $(X, Y, 0)$ *are mapped into* $(a_1 X, a_2 Y, 0)$*,* a_1*,* $a_2 > 0$*.*

In analogy with the notation we introduced earlier, the curve $\mathbf{r}_0(S) = \mathbf{r}(0, 0, S)$ in the physical space will denote the centerline curve at the deformed state.

We now make the basic assumptions regarding the kinematics of the arm. These assumptions slightly generalize traditional Euler-Bernoulli postulates for rod theory in solid mechanics where now in-plane deformations of the cross sections are admissible.

Assumption 1. *For each $S_0 \in [0,1]$, the ellipse $\{(X,Y,S_0),\ X^2/a_0^2+Y^2/b_0^2 \leq 1\}$ representing the cross section of the arm at S_0, is mapped onto an ellipse centered at $\mathbf{r}_0(S_0)$.*

Assumption 2. *The ellipse containing the points $\mathbf{r}(X,Y,S_0)$ is perpendicular to the deformed centerline at $\mathbf{r}_0(S_0)$, i.e.,*

$$(\mathbf{r}(X,Y,S_0)-\mathbf{r}_0(S_0))\cdot\frac{\mathrm{d}\mathbf{r}_0}{\mathrm{d}S}(S_0)=0 \tag{3.1}$$

for all X,Y.

Assumption 3. *Vectors in the plane $\{(X,Y,S_0)\}$ are mapped linearly to the plane of the ellipse at $\mathbf{r}_0(S_0)$, i.e., for each S_0 the mapping*

$$\mathbf{R}(X,Y,S_0)-\mathbf{R}_0(S_0)\mapsto(\mathbf{r}(X,Y,S_0)-\mathbf{r}_0(S_0)) \tag{3.2}$$

is linear.

Assumption 4. *The lines $\{(X,0,S_0)\}$ and $\{(0,Y,S_0)\}$ are mapped to the principal axes of the ellipse $\mathbf{r}(X,Y,S_0)$.*

We will naturally refer to the points $\mathbf{r}(X,Y,S_0)$ as the cross section of the deformed arm at S_0. Thus, Assumption 0 implies that the cross section at $S_0=0$, is not translated, rotated, or twisted. It is just stretched or contracted along the X and Y directions. Assumptions 1 and 2 are the classical assumption of rod theory that plane sections normal to the centerline remain plane and normal to the deformed centerline. Unlike the traditional Kirchhoff theory, we allow a cross section to deform in its plane, Assumption 3 implies that the in-plane deformation is homogeneous. In terms of the octopus's physiology, this implies uniform strain in the transverse fiber muscles. Furthermore, Assumption 4 implies that the X and Y are the principle axes of the in-plane linear strain, and as such, they remain perpendicular.

3.2. **The Centerline Triads.** For each point in the deformed arm, consider the base vectors

$$\mathbf{g}_p=\frac{\partial\mathbf{r}}{\partial X_p} \tag{3.3}$$

and note that

$$\mathbf{g}_p=\frac{\partial\mathbf{r}}{\partial X_p}=\frac{\partial\mathbf{r}}{\partial x_i}\frac{\partial x_i}{\partial X_p}=\frac{\partial x_i}{\partial X_p}\,\mathbf{e}_i. \tag{3.4}$$

The vector $\mathbf{g}_p$ at the point $\mathbf{r}_1=\mathbf{r}(\mathbf{R}_1)$ is tangent to the curve through $\mathbf{r}_1$ that contains the image of the curve $\mathbf{R}(X_p)=\mathbf{R}_1+X_{(p)}\mathbf{G}_{(p)}$ (no summation). Thus for example,

$$\mathbf{g}_3(0,0,S)=\frac{\partial\mathbf{r}}{\partial S}(0,0,S)=\frac{\mathrm{d}\mathbf{r}_0}{\mathrm{d}S}(S) \tag{3.5}$$

is the tangent (not necessarily of unit length) to the deformed centerline $\mathbf{r}_0(S)$. In addition, the vectors $\mathbf{g}_1$ and $\mathbf{g}_2$ are tangent to the cross section of the deformed arm.

From Assumptions 3 and 4 it follows that the base vectors $\mathbf{g}_1, \mathbf{g}_2$ are uniform and mutually perpendicular in any particular cross-section. In each elliptical cross section of the deformed arm, $\mathbf{g}_1$ and $\mathbf{g}_2$ are parallel to the principal axes. These two vectors represent the directions of the two mutually perpendicular transverse muscle groups in the deformed arm. By Assumption 2, $\mathbf{g}_3(0,0,S)$ is perpendicular to both $\mathbf{g}_1$ and $\mathbf{g}_2$. We conclude that the triads $\mathbf{g}_p(0,0,S)$ contain mutually orthogonal vectors. The vectors $\mathbf{g}_p(X,Y,S)$ at points other than the centerline need not be perpendicular. If, for example, the deformed arm becomes conical, the longitudinal fibers are no longer parallel. It is noted that the base vectors are not necessarily of unit length due to the centerline extension and the change in the principal axes of the elliptic cross-section.

We will refer to the triads $\mathbf{g}_p(0,0,S)$ as the centerline triads. It follows from Equation (3.4) that at each S there is a linear mapping $T(S)$ whose matrix is $\partial x_i/\partial X_p(0,0,S)$ such that

$$\mathbf{g}_p(0,0,S) = T(S)_{ip}\mathbf{e}_i. \tag{3.6}$$

It is recalled that according to the polar decomposition theorem, a non-singular linear mapping T may be decomposed in the form

$$T = Q \circ U \tag{3.7}$$

where Q is an orthogonal mapping and U is a positive definite symmetric mapping. Applying this to the mappings $T(S)$, so $T(S) = Q(S) \circ U(S)$, one can write for the centerline triads

$$\mathbf{g}_p(0,0,S) = Q(S)_{ij}U(S)_{jp}\mathbf{e}_i. \tag{3.8}$$

Each of the triads $\{\mathbf{d}_j(S)\}$, defined by

$$\mathbf{d}_j(S) = Q(S)_{ij}\mathbf{e}_i, \tag{3.9}$$

contains mutually orthogonal unit vectors. As the parameter S varies, the orthonormal triad rotates according to $Q(S)$ (see Figure 3.2). In our case, as the vectors $\mathbf{g}_p(0,0,S)$ are mutually orthogonal, the polar decomposition is particularly simple. The vectors $\mathbf{d}_j$ are simply the unit vectors in the directions of the vectors $\mathbf{g}_j$. The matrix Q_{ij} contains the components of $\mathbf{d}_j$ and the matrix U_{jp} is diagonal and contains the norms $\|\mathbf{g}_p\|$ of the vectors belonging to the centerline triad on its diagonal. The various $\{\mathbf{d}_i\}$ triads associated with the points $S \in [0,l]$ along the centerline, will be referred to as the *orthonormal rod frames*.

It follows that

$$\mathbf{d}_p(S) = \frac{1}{\|\mathbf{g}_p\|}\mathbf{g}_p(0,0,S) \quad \text{(no summation)}, \tag{3.10}$$

the unit vector $\mathbf{d}_3$ is tangent to the deformed centerline curve, and

$$\mathbf{g}_1(S) = a_1(S)\mathbf{d}_1(S), \quad a_1(S) = \|\mathbf{g}_1(0,0,S)\|, \tag{3.11}$$

$$\mathbf{g}_2(S) = a_2(S)\mathbf{d}_2(S), \quad a_2(S) = \|\mathbf{g}_2(0,0,S)\|. \tag{3.12}$$

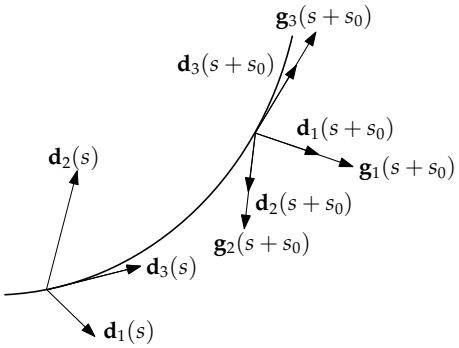

Figure 3.2: The triads $\{\mathbf{g}_i\}$ and $\{\mathbf{d}_i\}$, $i = 1, 2, 3$.

Using $\mathfrak{s}$ for the arc length parameter for the deformed centerline and assuming naturally that $\mathfrak{s}(S)$ is a monotonically increasing function, it follows from Equation (3.5) that the stretch or extension of the centerline is given by

$$\frac{\mathrm{d}\mathfrak{s}}{\mathrm{d}S}(S) = \|\mathbf{g}_3(0,0,S)\|. \tag{3.13}$$

We denote the stretch of the arm's centerline by $\lambda(S) = \|\mathbf{g}_3(0,0,S)\|$ and the length of the deformed centerline is $l = \int \lambda \mathrm{d}S$.

Using the centerline triads, our assumptions imply that the configuration of the arm may be represented by

$$\begin{aligned} \mathbf{r}(\mathbf{R}) &= \mathbf{r}_0(S) + X\mathbf{g}_1(0,0,S) + Y\mathbf{g}_2(0,0,S), \\ &= \mathbf{r}_0(S) + Xa_1(S)\mathbf{d}_1(S) + Ya_2(S)\mathbf{d}_2(S). \end{aligned} \tag{3.14}$$

3.3. **The Extended Darboux Vector.** As the parameter $\mathfrak{s}$ varies, the triad $\{\mathbf{d}_i\}$ undergoes a rigid motion. The origin of the triad is displaced tangent to the deformed centerline. The vectors $\mathbf{d}_i$ are rotated rigidly as expressed by Equation (3.9). As $\mathfrak{s}(S)$ was assumed to be monotonically increasing, one may consider the dependence $\mathbf{d}_i(\mathfrak{s}) = \mathbf{d}_i(S(\mathfrak{s}))$.

Consider the rates

$$\frac{\mathrm{d}\mathbf{d}_i}{\mathrm{d}\mathfrak{s}} = \frac{\mathrm{d}\mathbf{d}_i}{\mathrm{d}S}\frac{\mathrm{d}S}{\mathrm{d}\mathfrak{s}} = \frac{1}{\lambda}\frac{\mathrm{d}Q(S)_{ji}}{\mathrm{d}S}\mathbf{e}_j. \tag{3.15}$$

These rotation rates may be represented by a vector $\mathbf{u}$ so that,

$$\frac{\mathrm{d}\mathbf{d}_i}{\mathrm{d}\mathfrak{s}} = \mathbf{u} \times \mathbf{d}_i. \tag{3.16}$$

The components of $\mathbf{u}$ may be found by dot multiplying (3.16) by $\mathbf{d}_j$ obtaining

$$\frac{\mathrm{d}\mathbf{d}_i}{\mathrm{d}\mathfrak{s}} \cdot \mathbf{d}_j = (\mathbf{u} \times \mathbf{d}_i) \cdot \mathbf{d}_j. \tag{3.17}$$

Using ϵ_{ijk} to denote the permutation symbol, we have

$$\frac{\mathrm{d}\mathbf{d}_i}{\mathrm{d}\mathfrak{s}} \cdot \mathbf{d}_j = u_m \epsilon_{ijm}, \qquad u_m = \frac{1}{2}\epsilon_{ijm}\frac{\mathrm{d}\mathbf{d}_i}{\mathrm{d}\mathfrak{s}} \cdot \mathbf{d}_j. \tag{3.18}$$

It is straightforward to write similar expressions for the rates relative to the parameter S and write the relations between the two types of rates.

It is customary in rod theory (see [14]) to denote the components of the vector $\mathbf{u}$ as $\{\kappa, \kappa', \tau\}^T$ so

$$\begin{Bmatrix} \kappa \\ \kappa' \\ \tau \end{Bmatrix} = \begin{Bmatrix} u_1 \\ u_2 \\ u_3 \end{Bmatrix} = \begin{Bmatrix} \dfrac{\mathrm{d}\mathbf{d}_2}{\mathrm{d}\mathfrak{s}} \cdot \mathbf{d}_3 \\ \dfrac{\mathrm{d}\mathbf{d}_3}{\mathrm{d}\mathfrak{s}} \cdot \mathbf{d}_1 \\ \dfrac{\mathrm{d}\mathbf{d}_1}{\mathrm{d}\mathfrak{s}} \cdot \mathbf{d}_2 \end{Bmatrix}. \tag{3.19}$$

Denoting differentiation with respect to S by a prime, we immediately get by the chain rule

$$\mathbf{d}_i' = \lambda \frac{\mathrm{d}\mathbf{d}_i}{\mathrm{d}\mathfrak{s}} = \lambda \mathbf{u} \times \mathbf{d}_i. \tag{3.20}$$

The linear mapping $\mathbf{\Omega}$ defined by

$$\mathbf{\Omega}(\mathbf{v}) = \lambda \mathbf{u} \times \mathbf{v} \tag{3.21}$$

is represented by the matrix

$$\lambda \begin{bmatrix} 0 & \tau & -\kappa' \\ -\tau & 0 & \kappa \\ \kappa' & -\kappa & 0 \end{bmatrix}. \tag{3.22}$$

Thus, one has

$$\begin{Bmatrix} \mathbf{d}_1' \\ \mathbf{d}_2' \\ \mathbf{d}_3' \end{Bmatrix} = \mathbf{\Omega} \begin{Bmatrix} \mathbf{d}_1 \\ \mathbf{d}_2 \\ \mathbf{d}_3 \end{Bmatrix}. \tag{3.23}$$

The components of the vector $\mathbf{u}$ may be interpreted as follows: κ, κ' represent the bending of the centerline about the axes $\mathbf{d}_1$ and $\mathbf{d}_2$, respectively, and τ is the torsion about the tangent to the curve, $\mathbf{d}_3$. The parameter τ is different from the intrinsic torsion of the deformed centerline (described in the ~~next subsection~~appendix) as it accounts for the relative twist of the various cross sections of the arm. In addition, while the intrinsic torsion of a curve is not defined for the case where the curvature vanishes (see next subsection), τ is always well defined. It is noted that the rotation rate vector $\mathbf{u}$ is an extension of the Darboux vector used in differential geometry.

From the representation of the configuration in Equation (3.14), as the centerline triads may be obtained from their derivatives through integration and using the initial conditions given by Assumption 0, we conclude that the collection of function $\{\kappa(S), \kappa'(S), \tau(S), \lambda(S), a_1(S), a_2(S)\}$, defines uniquely the configuration of an extensible rod under the assumptions mentioned earlier. For example,

$$\mathbf{r}_0(S) = \int_{\sigma=0}^{S} \lambda(\sigma)\mathbf{d}_3(\sigma)\mathrm{d}\sigma. \tag{3.24}$$

3.4. ~~Representation of the Arm's Configuration Using the Frenet-Serret Parameters~~Moved to the Appendix.

4. The Deformation Gradient and Strain

4.1. **The Matrix of the Deformation Gradient.** Equation (3.14) for the description of the configuration determines the position vector in the deformed state of a particle having reference coordinates $(X,\, Y,\, S)$ by

$$\mathbf{r}(X,\, Y,\, S) = x_i \mathbf{e}_i = \mathbf{r}_0(S) + X\mathbf{g}_1(0,0,S) + Y\mathbf{g}_2(0,0,S).$$

We recall that the deformation gradient of solid mechanics, is the linear mapping

$$\mathbf{F} = F_{ip}\mathbf{e}_i \otimes \mathbf{G}_p. \tag{4.1}$$

represented by the matrix

$$F_{ip} = \frac{\partial x_i}{\partial X_p}\,. \tag{4.2}$$

Thus, the first two columns of the deformation gradient matrix are given by

$$F_{i1}\mathbf{e}_i = \frac{\partial \mathbf{r}}{\partial X} = \mathbf{g}_1, \tag{4.3}$$

$$F_{i2}\mathbf{e}_i = \frac{\partial \mathbf{r}}{\partial Y} = \mathbf{g}_2, \tag{4.4}$$

and the third column is given by

$$\begin{aligned} F_{i3}\mathbf{e}_i &= \frac{\partial \mathbf{r}_0}{\partial S} + X\frac{\partial \mathbf{g}_1}{\partial S} + Y\frac{\partial \mathbf{g}_2}{\partial S} \\ &= \lambda \mathbf{d}_3 + X\left(\frac{\mathrm{d}a_1}{\mathrm{d}S}\mathbf{d}_1 + a_1\frac{\mathrm{d}\mathbf{d}_1}{\mathrm{d}S}\right) + Y\left(\frac{\mathrm{d}a_2}{\mathrm{d}S}\mathbf{d}_2 + a_2\frac{\mathrm{d}\mathbf{d}_2}{\mathrm{d}S}\right). \end{aligned} \tag{4.5}$$

For any particular S, one may choose the basis $\{\mathbf{e}_i\}$ in space to be identical to the triad $\{\mathbf{d}_i(S)\}$. Under this specific choice, the last expressions imply that the matrix of $\mathbf{F}(X,Y,S)$ assumes the form

$$[\mathbf{F}]_{\mathbf{d}}\,(X,Y,S) = \begin{bmatrix} a_1 & 0 & \frac{\mathrm{d}a_1}{\mathrm{d}S}X - \tau\, a_2\lambda Y \\ 0 & a_2 & \tau\, a_1\lambda X + \frac{\mathrm{d}a_2}{\mathrm{d}S}Y \\ 0 & 0 & \lambda - \kappa' a_1\lambda X + \kappa a_2\lambda Y \end{bmatrix}, \tag{4.6}$$

where the dependence of the various variables on S was omitted on the right.

4.2. **The Consequences of Incompressibility.** As mentioned in Section 2, the octopus's arm is almost entirely composed of virtually incompressible muscle tissue. Indeed, in earlier treatments of Octopus arm kinematics (*e.g.*, [13]) it is assumed that the arm is incompressible. For the sake of simplicity, we assume the incompressibility constraint holds for segments of the arm rather than pointwise. A theoretical treatment of rod theory where the rod is assumed to be pointwise incompressible, was presented only recently in [11]. Thus, we make

Assumption 5. *The volume of any segment,* $\{(X,Y,S)\}$, $0 \le S_1 \le S \le S_2 \le 1$, *of the arm does not change under deformation.*

It is noted that for a pointwise incompressibility constraint the in-plane deformation of a cross section is not homogeneous (see [11]). Thus, pointwise incompressibility requirement would be inconsistent with our earlier assumptions.

Consider a volume element $\mathrm{d}V_0$ containing a material point $\mathbf{R}$ and its image $\mathrm{d}V$ containing $\mathbf{r}(\mathbf{R})$. Then, using J, the determinant of the deformation gradient, one has $\mathrm{d}V/\mathrm{d}V_0 = J$. The volume V of a deformed segment of the arm is thus given as

$$\begin{aligned} V &= \iiint J\,\mathrm{d}X\mathrm{d}Y\mathrm{d}S\,, \\ &= \int_{S_1}^{S_2} a_1(S)a_2(S)\lambda(S)\pi a_0 b_0\,\mathrm{d}S\,. \end{aligned} \tag{4.7}$$

Assuming that the integrand in Equation (4.7) is continuous, we conclude that a necessary and sufficient condition for the volume of every segment of the arm to remain unchanged, *i.e.,* that $V = V_0 = \pi a_0 b_0 (S_2 - S_1)$, is,

$$\lambda(S) = \frac{1}{a_1(S)\,a_2(S)}, \quad \forall S \in [0,1]. \tag{4.8}$$

Since the last equation cannot determine a unique pair (a_1, a_2) we make the following

Assumption 6. *The arm preserves the initial ratio between the lengths of the principal axes of the elliptic cross-section.*

We denote the above mentioned ratio as $r := \frac{a_0}{b_0}$. Consequently, $\frac{a_0}{b_0} = \frac{a_1 a_0}{a_2 b_0}$, and so, $a_1(S) = a_2(S) = \mathfrak{a}(S)$.

4.3. **Strain Analysis.** Consider an infinitesimal vector

$$\mathrm{d}\mathbf{X} = \mathrm{d}X_p \mathbf{G}_p \tag{4.9}$$

originating at the point $\mathbf{R}$ in the reference configuration, whose image under the deformation is

$$\mathrm{d}\mathbf{x} = \mathrm{d}x_i \mathbf{e}_i = \frac{\partial x_i}{\partial X_p}\mathrm{d}X_p \mathbf{e}_i = \mathbf{F}(\mathrm{d}\mathbf{X}) \tag{4.10}$$

originating at $\mathbf{r}(\mathbf{R})$. It is convenient, and indeed of wide use in the mechanics of continuous media, to describe the extension of the element $\mathrm{d}\mathbf{X}$ by the quantity

$$\frac{1}{2}\left[\mathrm{d}\mathbf{x}\cdot\mathrm{d}\mathbf{x} - \mathrm{d}\mathbf{X}\cdot\mathrm{d}\mathbf{X}\right] = \frac{1}{2}\left[\mathbf{F}^{\mathrm{T}}\mathbf{F} - \mathbf{I}\right](\mathrm{d}\mathbf{X})\cdot\mathrm{d}\mathbf{X} = \mathbf{E}\,(\mathrm{d}\mathbf{X})\cdot\mathrm{d}\mathbf{X}, \tag{4.11}$$

where,

$$\mathbf{E} = \frac{1}{2}\left[\mathbf{F}^{\mathrm{T}}\mathbf{F} - \mathbf{I}\right] \tag{4.12}$$

is the Lagrangian strain tensor.

This standard definition may be motivated intuitively using the special case of small deformations superimposed on the reference deformation as

follows, ~~For the case where the deformed state of the arm can be obtained by superimposing a small displacement field on the reference configuration, and~~If the vector $\mathrm{d}\mathbf{X}$ is normalized to be of unit length, $\frac{1}{2}\left[\mathrm{d}\mathbf{x}\cdot\mathrm{d}\mathbf{x}-\mathrm{d}\mathbf{X}\cdot\mathrm{d}\mathbf{X}\right]$ is the linear approximation to the change in length of $\mathrm{d}\mathbf{X}$ during the deformation.

~~Thus~~Returning to the general case of large deformations, for a unit vector $\hat{\mathbf{n}}$, originating at (X,Y,S), it is natural to refer to

$$\epsilon_{\hat{\mathbf{n}}}(X,Y,S)=(\mathbf{E}(X,Y,S)\hat{\mathbf{n}})\cdot\hat{\mathbf{n}} \tag{4.13}$$

as the *strain* at the point (X,Y,S) *in the direction* of $\hat{\mathbf{n}}$.

Once again, the Lagrangian strain tensor has a simpler expression when written relative to the orthonormal rod frame, and we have

$$[\mathbf{E}]_{\mathbf{d}}=\frac{1}{2}\begin{bmatrix}\mathfrak{a}^2-1 & 0 & \mathfrak{a}\left(\frac{\mathrm{d}\mathfrak{a}}{\mathrm{d}S}X-\mathfrak{a}\lambda Y\tau\right)\\ 0 & \mathfrak{a}^2-1 & \mathfrak{a}\left(\frac{\mathrm{d}\mathfrak{a}}{\mathrm{d}S}Y+\mathfrak{a}\lambda X\tau\right)\\ \mathfrak{a}\left(\frac{\mathrm{d}\mathfrak{a}}{\mathrm{d}S}X-\mathfrak{a}\lambda Y\tau\right) & \mathfrak{a}\left(\frac{\mathrm{d}\mathfrak{a}}{\mathrm{d}S}Y+\mathfrak{a}\lambda X\tau\right) & (\mathfrak{a}Y\lambda\kappa-\mathfrak{a}X\lambda\kappa'+\lambda)^2+\left(\frac{\mathrm{d}\mathfrak{a}}{\mathrm{d}S}Y+\mathfrak{a}\lambda X\tau\right)^2+\left(\frac{\mathrm{d}\mathfrak{a}}{\mathrm{d}S}X-\mathfrak{a}\lambda Y\tau\right)^2-1\end{bmatrix}. \tag{4.14}$$

It is noted that for $X=Y=0$, the mapping $\mathbf{F}$ becomes that mapping T of Equation (3.6). The strain $\mathbf{E}$ at the centerline is given by $(U^T\circ U-I)/2=(T^T\circ T-I)/2$, where U is the positive definite component of the decomposition in Equation (3.7).

5. Manipulator Kinematic Analysis

In this section we consider the octopus's arm as a manipulator and we study its kinematic properties, specifically, the inverse and direct kinematics. In order to perform such an analysis, one has to define what parameters of the configurations should be controlled. The arm is used as a tool along its entire length and the objective is to bring the suction elements into contact with some surface in such a way that the arm and the surface are tangent along the contact line. Thus, the manipulator kinematic analysis will consider the control of the configuration of the arm as described by the deformed centerline and generalized Darboux vector (rather than just the end of the arm or a segment of the arm, for example). Specifically, such a configuration will be given by the set of functions $\{\kappa(\mathfrak{s}),\kappa'(\mathfrak{s}),\tau(\mathfrak{s}),\lambda(S)\}$, where Equation (4.8) and Assumption 6 relate the extension parameter, $\lambda(S)$, with the cross-section parameter $\mathfrak{a}(S)$.

5.1. **Inverse Kinematics.**

For the inverse kinematics problem the configuration of the Octopus's arm is given in terms of the functions $\kappa(\mathfrak{s})$, $\kappa'(\mathfrak{s})$, $\tau(\mathfrak{s})$, $\lambda(S)$, and the actuation variables are the strains in the various muscle groups. It will be assumed that the fibers of the various groups are present

coincidently at all points in the arm. Accordingly, we will calculate the strains at each point in the arm in the directions of the various groups.

We set ϵ_L, ϵ_{T1}, ϵ_{T2}, ϵ_{H1}, ϵ_{H2} to be the strains in the directions of the longitudinal, oral-aboral and lateral transversal, and right and left helicoidal groups, respectively. Thus,

$$\begin{aligned} \epsilon_L &= \mathbf{d}_3 \cdot \mathbf{E}(\mathbf{d}_3), \\ \epsilon_{T1} &= \mathbf{d}_1 \cdot \mathbf{E}(\mathbf{d}_1), \\ \epsilon_{T2} &= \mathbf{d}_2 \cdot \mathbf{E}(\mathbf{d}_2), \\ \epsilon_{H1} &= \hat{\mathbf{n}}_c \cdot \mathbf{E}(\hat{\mathbf{n}}_c), \\ \epsilon_{H2} &= \hat{\mathbf{n}}_{cc} \cdot \mathbf{E}(\hat{\mathbf{n}}_{cc}), \end{aligned} \tag{5.1}$$

where $\hat{\mathbf{n}}_c$ and $\hat{\mathbf{n}}_{cc}$ are unit vectors pointing at the directions of the right and left coiled helicoidal muscle fibers, respectively. It assumed that in the reference configuration the helicoidal fibers are at 45° angle to the centerline[2]. Thus,

$$\begin{aligned} \hat{\mathbf{n}}_c &= \left\{ -\frac{rY}{A}, \frac{r^{-1}X}{A}, \frac{1}{\sqrt{2}} \right\}^T, \\ \hat{\mathbf{n}}_{cc} &= \left\{ \frac{rY}{A}, -\frac{r^{-1}X}{A}, \frac{1}{\sqrt{2}} \right\}^T, \end{aligned} \tag{5.2}$$

where $A = \sqrt{2}\sqrt{r^2Y^2 + r^{-2}X^2}$, and $r := a_0/b_0$ was defined following Assumption 6.

It is noted that by Assumption 6, $\epsilon_{T1} = \epsilon_{T2}$, and so it is natural to define the vector field

$$\boldsymbol{\epsilon}(X, Y, S) = \{\epsilon_{T1}(X, Y, S), \epsilon_L(S), \epsilon_{H1}(X, Y, S), \epsilon_{H2}(X, Y, S)\}^T \tag{5.3}$$

that contains the values of the analog of the actuation variables controlling the configuration of the arm.

For the inverse kinematics problem we seek a mapping Ψ that acts on the set of functions $\{\kappa(\mathfrak{s}), \kappa'(\mathfrak{s}), \tau(\mathfrak{s}), \lambda(S)\}$ and gives $\boldsymbol{\epsilon}$, so,

$$\boldsymbol{\epsilon}(X, Y, S) = \Psi(\kappa(\mathfrak{s}), \kappa'(\mathfrak{s}), \tau(\mathfrak{s}), \lambda(S), X, Y, S). \tag{5.4}$$

By using Equation (4.13) we find that,

$$\begin{Bmatrix} \epsilon_{T1} \\ \epsilon_L \\ \epsilon_{H1} \\ \epsilon_{H2} \end{Bmatrix} = [\mathbf{A}] \begin{Bmatrix} E_{11} \\ E_{33} \\ E_{13} \\ E_{23} \end{Bmatrix}, \tag{5.5}$$

where

$$[\mathbf{A}] = \begin{bmatrix} 1 & 0 & 0 & 0 \\ 0 & 1 & 0 & 0 \\ \frac{1}{2} & \frac{1}{2} & -\sin\theta & \cos\theta \\ \frac{1}{2} & \frac{1}{2} & \sin\theta & -\cos\theta \end{bmatrix}, \tag{5.6}$$

[2]The generalization to any other pitch angle is straightforward.

$\sin\theta = \frac{a_0^2 Y}{\sqrt{b_0^4 X^2 + a_0^4 Y^2}}$, and $\cos\theta = \frac{b_0^2 X}{\sqrt{b_0^4 X^2 + a_0^4 Y^2}}$.

We define a non-linear function $\mathbf{h}$ that takes the configuration parameters and gives the four strain components $(E_{11}, E_{33}, E_{13}, E_{23}) = \mathbf{h}(\kappa, \kappa', \tau, \lambda)$. By Equation (4.14) we have

$$\mathbf{h}(\kappa,\kappa',\tau,\lambda) = \frac{1}{2}\begin{Bmatrix} \mathfrak{a}^2 - 1 \\ (\mathfrak{a}\lambda\kappa Y - \mathfrak{a}\lambda\kappa' X + \lambda)^2 + (\mathfrak{a}' Y + \mathfrak{a}\lambda\tau X)^2 + (\mathfrak{a}' X - \mathfrak{a}\lambda\tau Y)^2 - 1 \\ \mathfrak{a}\mathfrak{a}' X - \tau Y \\ \mathfrak{a}\mathfrak{a}' Y + \tau X \end{Bmatrix}. \tag{5.7}$$

Hence, the inverse kinematics mapping Ψ is given by

$$\Psi = \mathbf{A} \circ \mathbf{h}. \tag{5.8}$$

5.2. **Forward Kinematics.** The forward kinematic problem is concerned with the inverse $\Phi = \Psi^{-1}$ of the mapping Ψ defined above. Since the analogs of the joint parameters in our case are the strain fields within the arm, ~~In the extreme case~~ one might expect that the domain on which Ψ is defined is the collection of all continuous independent strain fields

$$\{(E_{11}(X,Y,S), E_{33}(X,Y,S), E_{13}(X,Y,S), E_{23}(X,Y,S))\}. \tag{5.9}$$

However, this cannot hold true becausenot all strain fields correspond to continuous configurations of the arms. In fact, if a tensor field F_{ij} is indeed the gradient of a configuration of the arm, i.e., $F_{ij} = \partial x_i / \partial X_j$, then it must satisfy the compatibility condition~~of the compatibility restriction~~

$$\frac{\partial F_{ij}}{\partial X_p} = \frac{\partial F_{ip}}{\partial X_j} = \frac{\partial^2 x_i}{\partial X_j \partial X_p}. \tag{5.10}$$

~~for the corresponding deformation gradient.~~ Furthermore, it is clear that a generic configuration induced by a compatible strain field need not satisfy necessarily the assumptions we made in Subsection 3.1.For example, not every continuous configuration of the arm necessarily satisfies our assumption that the cross sections remain plane and perpendicular to the centerline. ~~For example~~Furthermore, using Equation (4.14) we find thatthe strain fields satisfy the constraint

$$E_{13} X + E_{23} Y = \mathfrak{a} \frac{\mathrm{d}\mathfrak{a}}{\mathrm{d}S}(X^2 + Y^2). \tag{5.11}$$

Thus, our analysis of the forward kinematics of the arm will lead us to the conclusion that the values of the strain at two points (X_1, Y_1, S_0), (X_2, Y_2, S_0) in a cross section S_0, that are not on the centerline, determine the values of $\mathfrak{a}(S_0)$, $\mathrm{d}\mathfrak{a}/\mathrm{d}S(S_0)$, $\kappa(\mathfrak{s}_0)$, $\kappa'(\mathfrak{s}_0)$, $\tau(\mathfrak{s}_0)$ and $\lambda(S_0)$, with some additional consistency conditions.

Noticing that the transformation $\mathbf{A}$ is singular and using

$$\frac{\mathrm{d}E_{11}}{\mathrm{d}S} = \frac{\mathrm{d}}{\mathrm{d}S}\frac{1}{2}(\mathfrak{a}^2 - 1) = \mathfrak{a}\mathfrak{a}' \tag{5.12}$$

and $\epsilon_{T1} = E_{11}$, we have

$$\begin{Bmatrix} \epsilon_{T1} \\ \epsilon_L \\ \epsilon_{H1} \\ \frac{\mathrm{d}\epsilon_{T1}}{\mathrm{d}S} \end{Bmatrix} = \begin{bmatrix} 1 & 0 & 0 & 0 \\ 0 & 1 & 0 & 0 \\ \frac{1}{2} & \frac{1}{2} & -\sin\theta & \cos\theta \\ 0 & 0 & \frac{X}{X^2+Y^2} & \frac{Y}{X^2+Y^2} \end{bmatrix} \begin{Bmatrix} E_{11} \\ E_{33} \\ E_{13} \\ E_{23} \end{Bmatrix}, \tag{5.13}$$

where now the transformation is invertible.

The inverse of Equation (5.13) will give the vector $\{E_{11}, E_{33}, E_{13}, E_{23}\}$ in terms of the modified strain functions vector, $\{\epsilon_{T1}, \epsilon_L, \epsilon_{H1}, \frac{\mathrm{d}\epsilon_{T1}}{\mathrm{d}S}\}$. In order to represent the configuration parameters $\{\kappa, \kappa', \tau, \lambda, a_1, a_2\}$ in terms of the strain functions—the forward kinematics mapping—, we use Equation (4.14) together with Equation (5.13) to obtain

$$a_1 = a_2 = \mathfrak{a} = \sqrt{2\epsilon_{T1} + 1}, \tag{5.14}$$

$$\tau = \frac{(a_0^2 - b_0^2)XY}{b_0^2X^2 + a_0^2Y^2}\epsilon'_{T1} + \frac{\sqrt{b_0^4X^2 + a_0^4Y^2}}{2(b_0^2X^2 + a_0^2Y^2)}\left(2\epsilon_{H1} - \epsilon_{T1} - \epsilon_L\right), \tag{5.15}$$

$$\kappa\mathfrak{a}Y - \kappa'\mathfrak{a}X = \frac{\sqrt{2\epsilon_L - (\mathfrak{a}'Y + \mathfrak{a}\tau\lambda X)^2 - (\mathfrak{a}'X - \mathfrak{a}\tau\lambda Y)^2 + 1}}{\lambda} - 1. \tag{5.16}$$

Since none of the configuration parameters are functions of X or Y, we find that the expressions on the right hand sides of Equations (5.14) and (5.15) depend only on S. Thus, the independence of these expressions on X and Y, originating from the kinematical assumptions made, may be used as conditions for the in-plane strain fields to be compatible with some configuration.

To find τ, κ, and κ', we evaluate Equations (5.15) and (5.16) at two points in a cross-section. For simplicity, we choose to evaluate the strain functions in Equation (5.15) at $X = a_0$, $Y = 0$, and thus we obtain,

$$\tau(S) = \frac{1}{a_0}\big(2\epsilon_{H1}(a_0, 0, S) - \epsilon_{T1}(a_0, 0, S) - \epsilon_L(a_0, 0, S)\big). \tag{5.17}$$

Setting $X = 0$, $Y = b_0$, and $X = a_0$, $Y = 0$, alternatively in Equation (5.16), we obtain

$$\kappa(S) = \frac{\sqrt{2\epsilon_L(0, b_0, S) - \big(\mathfrak{a}'^2(S) + \tau^2(S)\lambda(S)\big)b_0^2 + 1} - \lambda(S)}{\mathfrak{a}(S)\lambda(S)b_0}, \tag{5.18}$$

$$\kappa'(S) = \frac{\lambda(S) - \sqrt{2\epsilon_L(a_0, 0, S) - \big(\tau^2(S)\lambda(S) + \mathfrak{a}'^2(S)\big)a_0^2 + 1}}{\mathfrak{a}(S)\lambda(S)a_0}. \tag{5.19}$$

To conclude, we recall from Equation (4.8) that

$$\lambda(S) = \frac{1}{\mathfrak{a}^2(S)}. \tag{5.20}$$

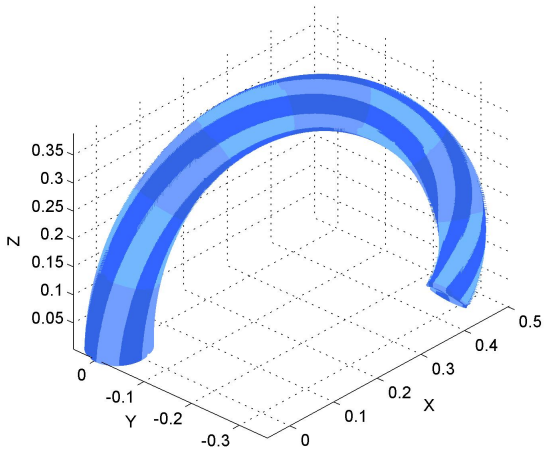

Figure 6.1: Illustration of the arm's configuration depicted by Equation 6.1

6. Example

To demonstrate the use of the model in computing the strains in the different muscle fibers, we consider the following configuration of the arm,

$$\kappa(S) = 5S, \quad \kappa'(S) = 2.7, \quad ,\tau(S) = 0.5S, \quad \lambda(S) = 1, \tag{6.1}$$

illustrated in Figure 6.1. By substituting Equation (6.1) into Equations (5.5), (5.6), we obtain the following strain field,

$$\begin{Bmatrix} \epsilon_{T1} \\ \epsilon_L \\ \epsilon_{H1} \\ \epsilon_{H2} \end{Bmatrix} = \begin{Bmatrix} 0 \\ \frac{1}{2}\left[(1 - 2.7X + 5SY)^2 + 0.25S^2(X^2 + Y^2) - 1\right] \\ \frac{1}{2}(\epsilon_L + 0.25\frac{(a_0^2Y^2 + b_0^2X^2)}{\sqrt{Y^2a_0^4 + X^2b_0^4}}S) \\ \frac{1}{2}(\epsilon_L - 0.25\frac{(a^2Y^2 + b^2X^2)}{\sqrt{Y^2a_0^4 + X^2b_0^4}}S) \end{Bmatrix}. \tag{6.2}$$

Computing the configuration parameters using Equations (5.14), (5.17)–(5.20) and the strains in (6.2), will result in the same configuration parameters given in Equation (6.1). Moreover, it is readily shown that Equation (5.16) holds for all $(X, Y) \in \{X = \alpha a_0,\, Y = \beta b_0 | \, 0 \leq \alpha \leq 1,\; 0 \leq \beta \leq 1\}$.

7. Conclusion

Studied from the point of view of robot kinematics. the octopus's arm emerges as a sophisticated continuous robot that uses the incompressibility of the material composing it in order to control its shape in space. We have no physiological data to support the assumption we have made regarding the behavior of the arm as a rod with variable cross section. In addition, we cannot justify our assumptions on the basis of the ratio between the size of the cross section relative to the length of the arm. Nevertheless, it seems to us that in the proposed model we were able to capture the essential aspects of the way the configuration of the arm is controlled. Hopefully, such analyses can inspire the constructions of efficient continuous robots.

References

[1] Y. Levinson, "On the kinematics of the octopus's arm", Master's thesis, Department of Mechanical Engineering, Ben-Gurion University, 2008.

[2] A. Cantino and G. Turk, "Arms: Physical simulation and control of muscular hydrostats", in *Neural Information Processing Systems*, 2005.

[3] F. Fahimi, H. Ashrafiuon, and C. Nataraj, "An improved inverse kinematic and velocity solution for spatial hyper-redundant robots", *IEEE Transactions on Robotics and Automation*, vol. 18, no. 1, pp. 103–107, 2002.

[4] B. A. Jones and I. D. Walker, "A new approach to Jacobian formulation for a class of multi-section continuum robots", in *Proceedings of the IEEE International Conference on Robotics and Automation*, 2005.

[5] B. A. Jones and I. D. Walker, "Kinematics for multisection continuum robots", *IEEE Transactions on Robotics*, vol. 22, pp. 43–55, 2006.

[6] Y. Yekutieli, R. Sagiv-Zohar, R. Aharonov, Y. Engel, B. Hochner, and T. Flash, "Dynamic model of the octopus arm I: Biomechanics of the octopus reaching movement", *Journal of Neurophysiology*, vol. 94, pp. 1443–1458, 2005.

[7] Y. Yekutieli, R. Sagiv-Zohar, B. Hochner, and T. Flash, "Dynamic model of the octopus arm II: Control of reaching movements", *Journal of Neurophysiology*, vol. 94, pp. 1459–1468, 2005.

[8] G. S. Chirikjian and J. W. Burdick, "Kinematically optimal hyper-redundant manipulator configurations", *IEEE Transactions on Robotics and Automation*, vol. 11, no. 6, pp. 794–806, 1995.

[9] K. E. Zanganeh and J. Angeles, "Inverse kinematics of hyper-redundant manipulators using splines", in *IEEE International Conference on Robotics and Automation*, 1995, vol. 3.

[10] F. Boyer, M. Porez, and W. Khalil, "Macro-continuous computed torque algorithm for a three-dimensional eel-like robot", *IEEE Transactions on Robotics*, vol. 22, no. 4, pp. 763–775, 2006.

[11] S. S. Antman, "A priori bounds on spatial motions of incompressible nonlinearly elastic rods", *Journal of Hyperbolic Differential Equations*, vol. 3, no. 3, pp. 481–504, 2006.

[12] W. M. Kier and K. K. Smith, "Tongues, tentacles and trunks: The biomechanics of movement in muscular-hydrostats", *Zoological Journal of Linnean Society*, vol. 83, pp. 307–324, 1985.

[13] W.M. Kier and M.P Stella, "The arrangement and function of octopus arm musculature and connective tissue", *Journal of Morphology*, vol. 268, pp. 831–843, 2007.

[14] P. Villaggio, *Mathematical Models for Elastic Structures*, Cambridge University Press, 1997.

[15] D. Struik, *Lectures on Classical Differential Geometry*, Addison-Wesley, 1961.

Appendix A. Representation of the Arm's Configuration Using the Frenet-Serret Parameters

An alternative approach to the above description of the arm's configuration is based on the well known Frenet-Serret parameters (FS) [15] for a spatial curve represented by a vector function, $\mathbf{r}_0(\mathfrak{s}) \in \mathbb{R}^3$, where $\mathfrak{s}$ is the arc length along the curve. It is recalled that for the case of non-vanishing curvature, a unique Frenet-Serret frame can be associated with each point on the curve. The Frenet-Serret orthonormal basis at a point S is given by,

$$\mathbf{T} = \frac{\mathrm{d}\mathbf{r}_0}{\mathrm{d}\mathfrak{s}}, \quad \mathbf{N} = \frac{1}{\kappa_{\mathrm{FS}}}\frac{\mathrm{d}\mathbf{T}}{\mathrm{d}\mathfrak{s}}, \quad \mathbf{B} = \mathbf{T} \times \mathbf{N}, \tag{A.1}$$

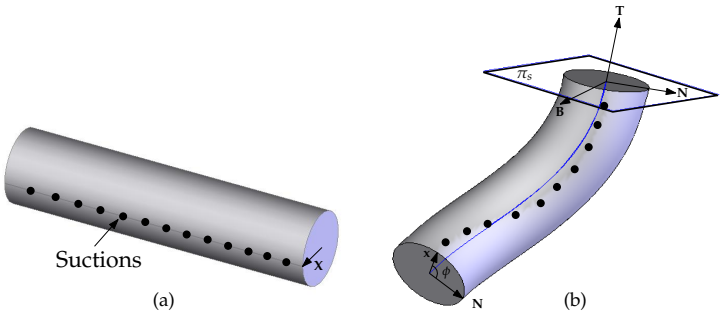

Figure A.1: (a) Reference configuration, (b) Current configuration.

where $\mathbf{T}$, $\mathbf{N}$ and $\mathbf{B}$ are referred to as the tangent, normal and bi-normal vectors, respectively. (We omitted the dependence on S for brevity.) The parameters κ_{FS}, the curvature, and τ_{FS}, the torsion, are defined by

$$\kappa_{\text{FS}} = \left\| \frac{\mathrm{d}\mathbf{T}}{\mathrm{d}\mathfrak{s}} \right\|, \qquad \tau_{\text{FS}} = \frac{\mathrm{d}\mathbf{N}}{\mathrm{d}\mathfrak{s}} \cdot \mathbf{B}. \tag{A.2}$$

It can be shown that the curvature function and the torsion function uniquely define an inextensible spatial curve up to a rigid body displacement [15]. The Frenet-Serret triads satisfy the differential equations

$$\begin{aligned} \frac{\mathrm{d}\mathbf{T}}{\mathrm{d}\mathfrak{s}} &= \kappa_{\text{FS}}\mathbf{N}, \\ \frac{\mathrm{d}\mathbf{N}}{\mathrm{d}\mathfrak{s}} &= -\kappa_{\text{FS}}\mathbf{T} + \tau_{\text{FS}}\mathbf{B}, \\ \frac{\mathrm{d}\mathbf{B}}{\mathrm{d}\mathfrak{s}} &= -\tau_{\text{FS}}\mathbf{N}. \end{aligned} \tag{A.3}$$

The Frenet-Serret triads describe the geometry of the deformed centerline. In order to describe the configuration of the arm completely, we need to account for the stretch λ, the in-plane deformation and the twist of the arm about the centerline. In order to describe the twist, we define a parameter ϕ, the angle between the normal unit vector $\mathbf{N}$ and the image, $\mathbf{g}_1$, of the vector $\mathbf{G}_1$ (see Figure A.1).

Given the set $\{\kappa,\, \kappa',\, \tau\}$, when $\kappa^2 + \kappa'^2 \neq 0$, one can find the corresponding F.S. parameters by,

$$\kappa_{\text{FS}} = \sqrt{\kappa'^2 + \kappa^2}, \tag{A.4}$$

$$\tau_{\text{FS}} = \tau + \frac{1}{(\kappa'^2 + \kappa^2)^{3/2}} \left(\kappa \frac{\mathrm{d}\kappa'}{\mathrm{d}\mathfrak{s}} - \kappa' \frac{\mathrm{d}\kappa}{\mathrm{d}\mathfrak{s}} \right), \tag{A.5}$$

$$\phi = \cos^{-1}\left(\frac{\kappa'}{\sqrt{\kappa'^2 + \kappa^2}} \right) = \sin^{-1}\left(\frac{-\kappa}{\sqrt{\kappa'^2 + \kappa^2}} \right). \tag{A.6}$$